INTERNATIONAL SOCIETY FOR SOIL MECHANICS AND GEOTECHNICAL ENGINEERING

Effect of Pipes Used as Advance Support Measure on the Development of Load-Bearing Ring of Soil

I. Bathaeian[1], B. Schneider-Muntau[2]

[1]*ILF Consulting Engineers Austria GmbH*

[2]*University of Innsbruck, Department of Geotechnical Engineering*

ABSTRACT: Pipes have long been used to support the crown in soft ground and avoid local degradation of soil strength and stiffness. The main role of the pipes is rather to preserve the geometric shape of the excavation rather than to carry loads themselves. In this way a load-bearing ring of soil around the tunnel can develop. The load-bearing effect is achieved by the development of arching effects in the soil between the individual pipes in the transverse and longitudinal directions. In order to evaluate this mechanism, model tests in a sandbox at a scale of 1:20 of a section of the system were carried out. The effects of grain size, density, and stress level were investigated. The displacements and arching effect between the pipes were visualized by particle image velocimetry. The main aim of this study is to analyse the arching effect by means of model tests and numerical calculations. The numerical calculations are conducted with different material models (Mohr-Coulomb, Hardening Soil, Hypoplasticity) and the results are compared.

Keywords: Shotcrete Tunnelling, Pipes, Mohr-Coulomb, Hardening Soil, Hypoplasticity

1 INTRODUCTION

In shotcrete tunnelling, various advance methods are used to support the tunnel cross-section and reduce settlements during excavation. The most common methods are pipe umbrellas, spiles, grouting and ground freezing (Maidl et al. 2014 and Pöttler et al. 2004). Approximately half of the tunnel excavation time (Grimmscheid 2008) is required for the installation of pipes. Therefore, reducing the construction time by optimising the pipe spacing will significantly increase the efficiency of this method. In this contribution an experimental and numerical set up is presented with the goal to investigate the bearing behaviour of pipes.

2 EXPERIMENTAL INVESTIGATIONS

2.1 Model Geometry

The model for the experimental investigations was constructed on a scale of 1:20, which in prototype corresponds to a tunnel with a diameter of almost 8 m. The external dimensions of the model are chosen so that the boundary effects have no to negligible influence on the results. The overburden of the model is limited to 1 m, which corresponds to 20 m overburden in the nature. The axial distance between the pipes in the model is set to 16 mm, which corresponds to an axial distance of 0.32 m in reality. For the Particle Image Velocimetry (PIV) measurements, a 30 mm thick acrylic glass is installed at the front of the model. The tunnel excavation is modelled by discharging the sand through an opening under the model. The geometry of the model is shown in Figure 1.

2.2 Material

The experiments were carried out with washed quartz Ottendorf-Okrilla sand with different grain size distributions. A fine sand with a grain size of 0.1 – 0.5 mm and a coarse sand with a grain size of 1.0 – 2.0 mm were used. The shear parameters of the partially saturated sand were determined by several laboratory tests with water content $\omega = 2\%$.

Figure 1. Model with a scale of 1:20 for experimental investigations (Pöchacker 2022)

2.3 Experiments with partially-saturated sand

In experiments with partially saturated sand (water content $\omega = 2\%$) and a variety of relative densities $D_r = 0.75 \sim 0.98$, a load bearing ring of soil is formed. This ring of soil only fails when the pipe spacing is increased by pulling out some of the pipes see Figure 2.

Figure 2. Arch formation between the pipes prior to failure, with $\omega = 2\%$ and $D_r = 0.98$, (Pöchacker 2022)
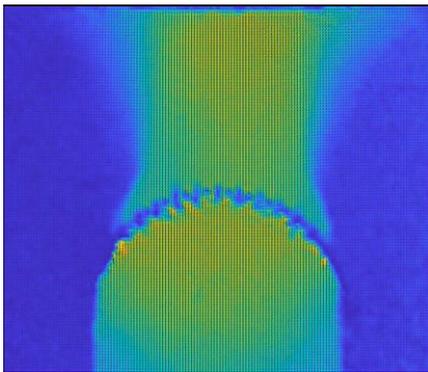

Figure 3. Pattern of displacement after discharging the model – PIV, with $\omega = 2\%$ and $D_r = 0.98$,(Pöchacker et al. 2022)

The evaluation of the experiments was performed with PIV, see Figure 3. For a detailed description of the experiments, comparison of the results with analytical solutions and PIV evaluations, see Pöchacker 2022 and Pöchacker et al. 2022.

3 NUMERICAL MODEL

The experiments are modelled using 3D finite element analysis (PLAXIS 3D). The dimensions of the model are chosen based on the geometry of the experimental model introduced in section 2.1. The first aim of the numerical calculation is to investigate the difference in the results when the pipes are modelled as continuum or with line elements, i.e. embedded beam or beam elements, see also Tschuchnigg 2015. For soil 10-node tetrahedral elements are created in the 3D mesh. The beam element and the embedded beam elements are used to model the semi-one-dimensional structural objects, i.e.

the pipes, with a bending stiffness. The embedded beam element is used to describe the interaction of semi-one-dimensional elements such as piles or rock bolts with the surrounding rock or soil. The finite element discretisation of the embedded beam element is very similar to that of the beam element, except that when embedded beam elements are modelled in a volume, three additional nodes are introduced within the volume to allow for the interaction with soil or rock. For more information on the formulation and discretisation of these elements, see Sadek & Shahrour 2004 and the Plaxis Scientific Manual.

3.1 Modelling the pipes as volume elements

Here the pipes are modelled as volume elements, see Figure 4a. The surface of the pipes is modelled either as smooth or rough. The smooth surface is modelled by creating a surface on the volume, where all displacements are set to free. The rough surface is modelled by creating an interface on the surface of the volume. The shear parameters of the interface are set to 2/3 of the shear parameters of the soil material. To fix the pipes at both ends, prescribed surface elements are set at both ends. On these surfaces all displacements are fixed. Therefore, rotation and displacement of the pipes are constrained.
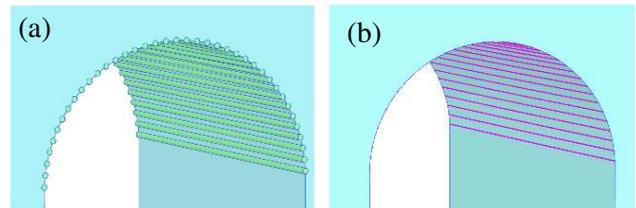

Figure 4. FE-model with pipes a) as volume elements and b) as beam or embedded beam

3.2 Modelling the pipes as line elements

Here the pipes are modelled as either beams or embedded beam elements, see Figure 4b. The beam element and the embedded beam element shall correspond to smooth and rough pipe surfaces, respectively. To fix the pipes at both ends, prescribed point elements are placed at both ends. At these points all displacements are fixed. Therefore, rotation and displacements of the pipes are constrained.

3.3 Calculation phases

The numerical modelling is carried out in three steps:

I. Direct generation of initial stresses using the K_0 procedure. The horizontal stress ratio is calculated with, $K_0 = 1 - \sin \varphi'$

II. Activation of the pipes and the prescribed fixities.

III. Tunnel excavation by deactivating the soil in the tunnel cluster, i.e. area of excavation.

3.4 Material model and parameters

The Mohr-Coulomb material model is used to investigate the differences for pipes modelled as continuum or as line elements. A series of direct shear tests were carried out on partially saturated Ottendorf-Okrilla sand. The tests were performed with dense and semi-dense sands. The shear parameters of compacted sand resulting in apparent cohesion and peak friction angle for different stress levels are given in (Pöchacker 2022). The parameters given in Table 1 are selected for this analysis.

Table 1. Mohr-Coulomb Parameters for FE-calculations

Elastic Modulus (kN/m²)	Poisson's Ratio (-)	Cohesion (kN/m²)	Peak friction Angle (°)
E	ν	c'	φ'
5000	0.2	5	33

4 COMPARISON OF MODELS WITH SMOOTH SURFACE

The results are compared for a section in the centre of the model to minimise boundary effects on the results.

4.1 Displacements

The comparison of the vertical displacements after excavation in Figure 5 in both models shows that the displacement in the pipe as a volume element (Figure 5a) is almost half of that in the model with pipes modelled as beam elements (Figure 5b). This significant difference in the displacements can be attributed to the fact that in the model with the volume elements as pipes, the real thickness of the pipes and, correspondingly, a smaller opening between the pipes is modelled.
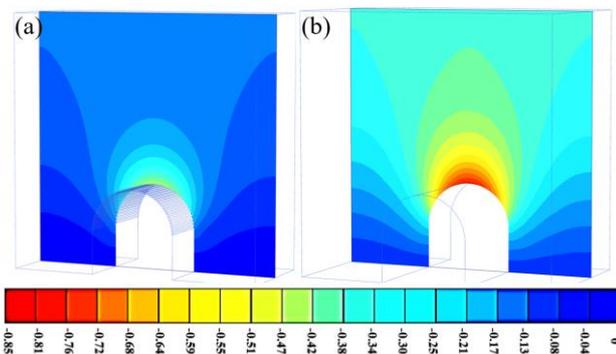

Figure 5. Vertical displacements in model with pipes as volume element (a) and in model with pipes as beam element (b), legend in mm

4.2 Arching effect in model with smooth surface

According to (Terzaghi 1943), the transfer of pressure from a yielding mass of soil to adjacent stationary parts is commonly referred to as the arching effect.
To demonstrate and compare the formation of the arching

effect between the pipes, the incremental deviatoric strains are shown in Figure 6 and the direction of the principal effective stress σ_1' is shown in Figure 7.
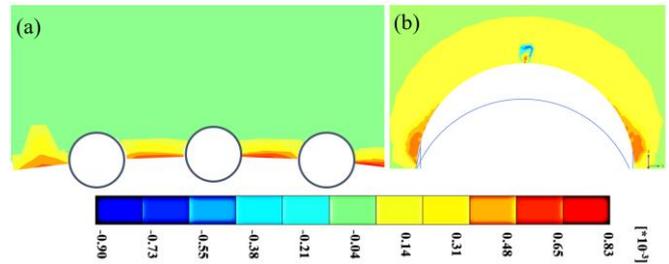

Figure 6. Incremental deviatoric strain in model with pipes as volume element (a) and in model with pipes as beam element (b)
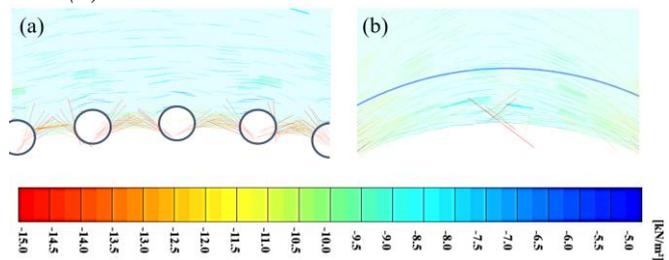

Figure 7. Direction of principal effective stress in model with pipes as volume (a) and in model with pipes as beam element (b)

As can be seen from the Figures 6 and 7, the arching between the pipes considered as volume elements is clearly visible and the beam element model is not able to reproduce the arching effect between the pipes.

5 COMPARISON OF MODELS WITH ROUGH SURFACE

5.1 Displacements

Similar to section 4.1, the comparison of vertical displacements for models with rough surfaces shows that the displacement in the model with pipes as volume elements are significantly smaller, see Figure 8.
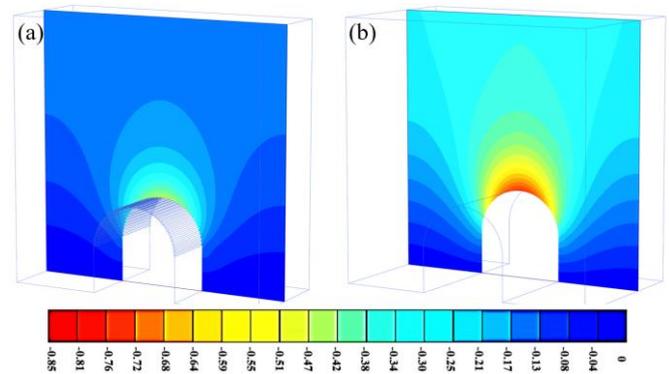

Figure 8. Vertical displacements in model with pipes as volume element (a) and with pipes as beam element (b), legend in mm

5.2 Arching effect in model with rough surface

To compare the formation of arches, only the direction of the principal effective stress σ_1' is compared in Figure 9. The embedded beam element, like the beam element, is not able to form an arch between the pipes.
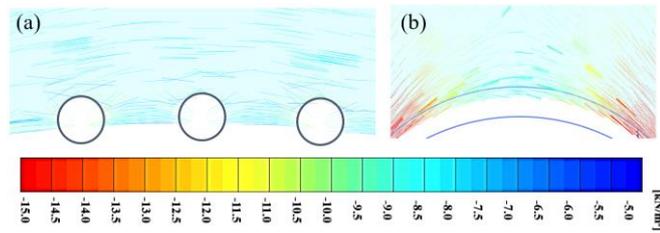

Figure 9. Direction of principal effective stress in model with pipes as volume (a) and as beam element (b)

6 HYPOPLASTIC AND ELASTOPLASTIC MODELLING

The model with pipes as volume elements with a smooth surface is chosen to compare the results between the hypoplastic and elastoplastic models. For this purpose, the hypoplastic model according to von Wolffersdorff 1996 and the Hardening Soil model (Schanz et al. 1999) are chosen. In the next two sections, the main characteristics of the chosen material models are discussed. The formulation and characteristics of these models has been extensively discussed in the relevant literature.

6.1 Hypoplastic Model

The main characteristics of hypoplastic models are listed here:
• Deformation is not divided into elastic and plastic parts. There is no plastic potential, yield surface, flow rule and consistency condition,
• Hypoplasticity includes the influence of stress level (barotropy) and the density (pyknotropy) on the behaviour of soil,
• Stiffness, changes in volume (dilatancy or contractancy) and mobilisation of the peak friction angle result from the actual stress state and density of the soil element and the direction of the deformation,
• Matsuoka-Nakai critical stress states

6.2 Hardening Soil Model

The hardening soil model (HS) has been developed as an advanced elastoplastic model in order to account for several soil characteristics such as:
• Stress-dependent stiffness according to a power law,
• Soil stress history and pre-consolidation effects,
• Dilatation,
• Failure according to the Mohr-Coulomb criterion.

6.3 Parameters

In (Marcher et al. 2000), the calibration of the hypoplastic and Hardening Soil material models for standard laboratory tests is carried out. The proposed parameters for dense and loose compaction of the Hostun sand are used for comparative calculations in this study.

Table 2. Parameters of the Hypoplastic model for Hostun-Sand, with φ_c the critical friction angle, h_s the granular hardness, n the exponent, e_{c0} and e_{d0} the critical and minimum void ratio at zero pressure.

φ_c (°)	h_s (MPa)	n	e_{c0}	e_{d0}	p_t (kPa)
32	1000	0.29	0.91	0.61	1

e_{i0}	α	β	e_i (dense)	e_i (loose)
1.09	0.19	2	0.63	0.90

Table 3. Parameters of the Hardening Soil model for Hostun-Sand – dense/loose compaction with φ'_p the peak friction angle, c' the cohesion, ψ' the dilatancy and E_{50}^{ref} and E_{oed}^{ref} stiffness and stiffness in oedometric compression.

φ'_p (°)	c' (kPa)	ψ' (°)	E_{50}^{ref} (MPa)	E_{oed}^{ref} (MPa)
44/34	0.6	14/0	30/12	30/16

m	E_{ur}^{ref} (MPa)	ν_{ur}
0.55/0.75	90/60	0.25

These parameters are given in Table 2 and Table 3. The parameter p_t in the hypoplastic model, which replaces the effective stress $\boldsymbol{\sigma}$ with $\boldsymbol{\sigma} - \mathbf{1}p_t$, is chosen equal to the default value of 1 kPa, as explained in (Mašín 2017). For the HS model, in order to facilitate convergence, a minimum cohesion of 0.6 kPa is similarly considered.
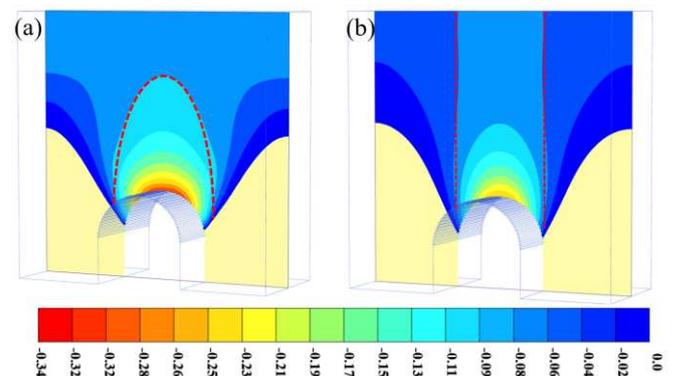
6.4 Results for dense sand

Figure 10. Vertical displacements for dense compaction between HS model (a) and hypoplastic model (b), legend in mm

The vertical displacements are shown in Figure 10. The magnitude of the calculated displacements with hypoplastic model is approximately 25% smaller than that with the HS model.

A comparison of the magnitude of the displacements with those obtained from the experiment is not possible, as these results are calculated for Hostun sand parameters, which is different from those used in experiments (no calibration available so far). However, it is worth comparing the pattern of the displacements with the PIV evaluation. The pattern of the displacements for the hypoplastic model shows a downward moving soil column with a diameter almost equal to the diameter of the tunnel. This result is in good agreement with the PIV evaluation, see Figure 3. On the other hand, the HS model results show a curved distribution of displacements above the tunnel crown.
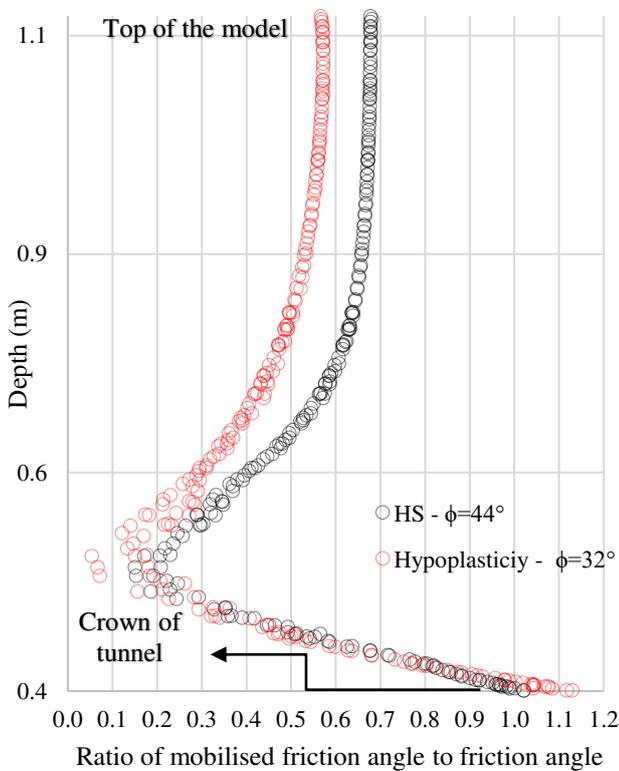

Figure 11. Ratio of mobilised friction angle to the friction angle at the centre of the tunnel crown – dense compaction

Along a line at the centre of the tunnel crown between two pipes, the ratio of the mobilised friction angle to the friction angle is calculated for the HS and hypoplasticity models, see Figure 11. The results show that for dense sand, the ratio of the mobilised friction angle for Hypoplasticity, near the tunnel crown, exceeds the value of 1, mainly due to the mobilisation of a peak friction angle. It is also evident that in the area of the arch (in the crown of the tunnel), the peak friction angle of HS is fully mobilised. The ratio of the mobilised friction angle decreases in both models up to a depth of almost 0.5 m and then begins to increase, reaching a value of 0.5 near to the top of the model.

6.5 Results for loose sand

The vertical displacements are shown in Figure 12. Similar to dense compaction calculations, the vertical displacements using hypoplasticity model are smaller. Loose compaction calculations also show the same difference in the pattern of displacement.
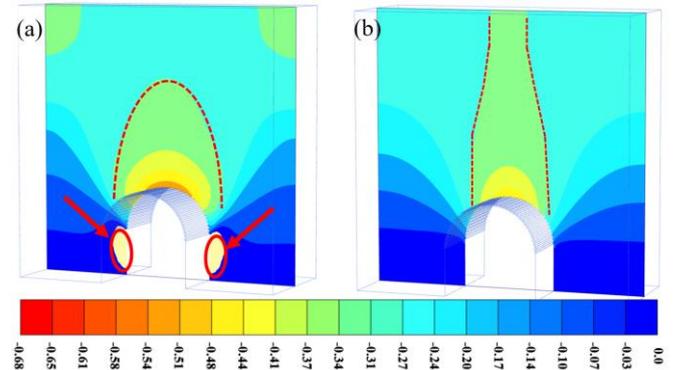

Figure 12. Vertical displacements for loose compaction between HS model (a) and Hypoplastic model (b), legend in mm

The red arrows in Figure 12a indicate the location of two zones, where the HS model results show slight upward displacements on either side of the tunnel walls.
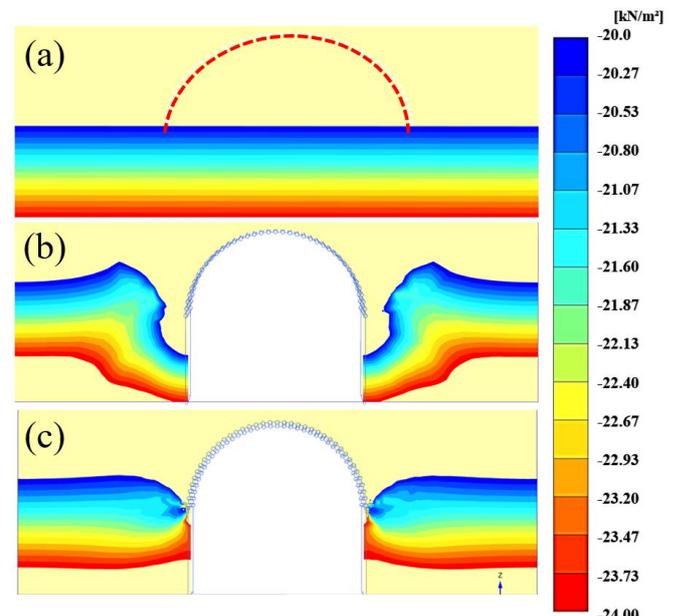

Figure 13. Initial vertical effective stress (a) – effective vertical stress after excavation for HS model (b) and hypoplasticity model (c)

This behaviour can be explained by the excessive reduction of effective stress in these zones by the HS model compared to hypoplasticity model. Figure 13 shows the redistribution of effective vertical stress in both models compared to the initial stress state. In Figure 14 the ratio of mobilised friction angle to friction angle is calculated for both models. The results show that due to the lack of dilatant behaviour and correspondingly lower interpipe

stress level, the maximum friction angle cannot be mobilised in either model. Compared to HS with a ratio of almost 0.85, the hypoplasticity results show a much lower mobilisation of the friction angle with a ratio of 0.3.
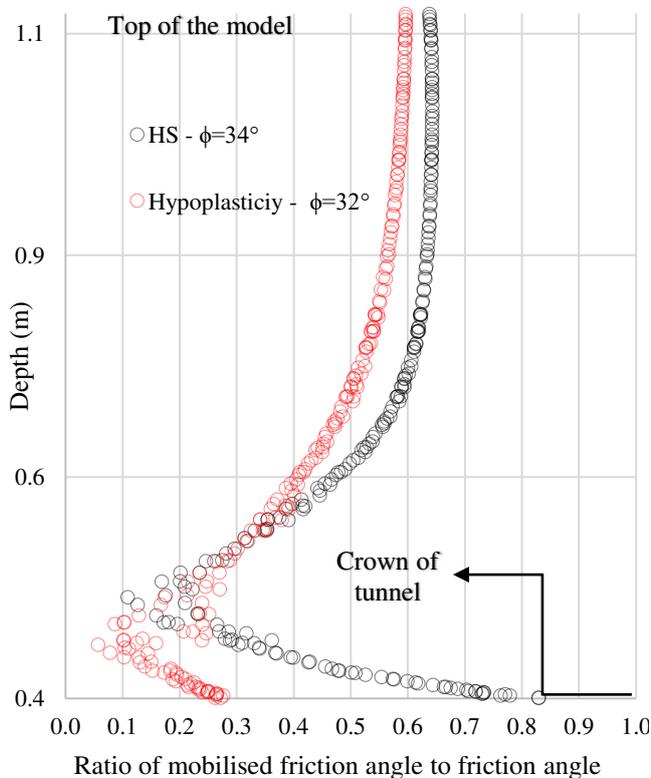

Figure 14. Ratio of mobilised friction angle to the friction angle at the centre of the tunnel crown – loose compaction

7 CONLUSION

This paper presents an experimental model for investigating of the effect of pipes used as an advance support measure in tunnelling. Although the stress state in the experimental model does not correspond to real conditions, the experiments clearly show the development of a supporting soil ring around the pipes.

A series of numerical back-calculations of the experiment are performed. The results show, firstly, that the arching effect is better reproduced when the pipes are modelled as volume elements. Secondly, comparative calculations with HS and Hypoplasticity show that for dense sand, the interpipe stresses are greater and correspondingly larger friction angles can be mobilised. It is also shown that the HS model overestimates the reduction in effective stress, resulting in upward movement in some areas of the model. Future work will include similar calculations for real tunnel geometries and larger overburden based on obtained insights of this study. These investigations are intended to eliminate the limitations of the present investigation with regard to the low stress state and the correspondingly low stiffness of the soil and simplified modelling of tunnel excavation.

9 REFERENCES

Bentley Advancing Infrastructure, Scientific Manual, PLAXIS, 2022.

Girmscheid, G., 2008, Baubetrieb und Bauverfahren im Tunnelbau , *2. Aufl. Berlin: Wiley.*

Marcher, Th., Vermeer, P. A., von Wolffersdorff, P.-A., 2000, Hypoplastic and elastoplastic modelling – a comparison with test data. *Constitutive modelling of granular materials*, Springer Berlin Heidelberg.

Maidl, B., Thewes, M., Maidl, U., 2014. Handbook of Tunnel Engineering II: Basics and Additional Services for Design and Construction. *John Wiley & Sons.*

Mašín, D., 2017, PLAXIS Implementation of Hypoplasticity

Pöchacker, C. 2022. *Experimentelle und numerische Untersuchungen zum Einfluss geometrischer Parameter auf den optimalen Spießabstand im Tunnelbau* , Universität Innsbruck, Austria.

Pöchacker, C.; Schweinberger, M.; Bathaeinan, I.; Schneider-Muntau, B. 2022: Experimentelle Untersuchungen zum Einfluss geometrischer Parameter auf den optimalen Spießabstand im Tunnelbau. Vorträge zum 28. Darmstädter Geotechnik-Kolloquium. Mitteilungen des Institutes für Geotechnik der Technischen Universität Darmstadt, Heft Nr. 113

Pöttler, R., Spiegl, A., Volkmann, G., Leitner, R., 2004: Lastabtragung an der Ortsbrust unter Berücksichtigung der Ortsbruststabilität und vorausleienden Sicherung. *Österreichischer Tunneltag 2004 und 53. Geomechanik Kolloquium*

Sadek, M., Shahrour, I., 2004. A three dimensional embedded beam element for reinforced geomaterials. *International Journal for Numerical and Analytical Methods in Geomechanics*, **28**, 931-946.

Schanz, T., Vermeer P. A., Bonnier P. Gc., 1999, The hardening soil model: formulation and verification. *Beyond 2000 in computational geotechnics*, Balkama, Rotterdam.

Terzaghi, K. 1943. *Theoretical Soil Mechanics*, John Wiley and Sons, INC., New York.

Tschuchnigg, F.; Schweiger, H. 2015, *The embedded pile concept – Verification of an efficient tool for modelling complex deep foundations*. Computers and Geotechnics, 63

von Wolffersdorff, P.-A., 1996, A hypoplastic relation for granular materials with predefined limit state surface. *Mechanics of Cohesive-frictional Materials: An International Journal on Experiments, Modelling and Computation of Materials and Structures*, Volume **1**, Issue 3.